

1 **Running Head:** Traits and performance landscapes

2

3 **Alternative designs and tropical tree seedling growth performance landscapes**

4

5 Samantha J. Worthy^{1,*}, Daniel C. Laughlin², Jenny Zambrano³, María Natalia Umaña⁴, Caicai
6 Zhang⁵, Luxiang Lin⁵, Min Cao⁵, and Nathan G. Swenson¹

7

8 ¹Department of Biology, University of Maryland, College Park, Maryland 20742, U.S.A.

9

10 ²Department of Botany, University of Wyoming, Laramie, WY 82071, U.S.A.

11

12 ³The School of Biological Sciences, Washington State University, Pullman, WA 99164, U.S.A

13

14 ⁴Department of Ecology and Evolutionary Biology, University of Michigan, Ann Arbor, MI
15 48109, U.S.A.

16

17 ⁵ CAS Key Laboratory of Tropical Forest Ecology, Xishuangbanna Tropical Botanical Garden,
18 Chinese Academy of Sciences, Kunming, Yunnan 650201, China

19

20 *Corresponding Author: Samantha J. Worthy; 1210 Biology Psychology Bldg., 4094 Campus Dr.
21 University of Maryland, College Park, MD, 20742; Telephone: +1-334-695-0136; E-mail:
22 sworthy@terpmail.umd.edu

23 **Abstract**

24 The functional trait values that constitute a whole-plant phenotype interact with the
25 environment to determine demographic rates. Current approaches often fail to explicitly consider
26 trait-trait and trait-environment interactions, which may lead to missed information that is
27 valuable for understanding and predicting the drivers of demographic rates and functional
28 diversity. Here, we consider these interactions by modeling growth performance landscapes that
29 span multidimensional trait spaces along environmental gradients. We utilize individual-level

This is the author manuscript accepted for publication and has undergone full peer review but has not been through the copyediting, typesetting, pagination and proofreading process, which may lead to differences between this version and the [Version of Record](#). Please cite this article as [doi: 10.1002/ECY.3007](https://doi.org/10.1002/ECY.3007)

This article is protected by copyright. All rights reserved

30 leaf, stem and root trait data combined with growth data from tree seedlings along soil nutrient
31 and light gradients in a hyper-diverse tropical rainforest. We find that multiple trait combinations
32 in phenotypic space (i.e. alternative designs) lead to multiple growth performance peaks that
33 shift along light and soil axes such that no single or set of interacting traits consistently results in
34 peak growth performance. Evidence from these growth performance peaks also generally
35 indicates frequent independence of above and below ground resource acquisition strategies.
36 These results help explain how functional diversity is maintained in ecological communities and
37 question the practice of utilizing a single trait or environmental variable, in isolation, to predict
38 the growth performance of individual trees.

39

40 Key Words: Demographic Rate, Forest Ecology, Functional Traits, Growth, Seedlings, Tropical
41 Forest

42 **Introduction**

43 The diversity and dynamics of communities are driven by differential demographic rates
44 that largely arise from how phenotypes interact with the environment (Fonseca et al. 2000,
45 Ackerly 2003, Cavender-Bares et al. 2004, HilleRisLambers et al. 2012, Anderson 2016). The
46 links between functional traits, demographic rates, and population and community structure form
47 the basis of trait-based community ecology (McGill et al. 2006). In this regard, two analytical
48 approaches are common: quantifying the relationships between single traits and demographic
49 rates, and quantifying the relationships between traits and environmental gradients (Wright and
50 Westoby 1999, Poorter et al. 2008, Enquist et al. 2015, Jager et al. 2015, Costa et al. 2017). The
51 first approach generally operates under the implicit assumption that trait-demographic rate
52 relationships are consistent across environments (Wright et al. 2004, Poorter et al. 2008, Kraft et
53 al. 2010, Adler et al. 2014). For example, a low wood density confers fast growth (e.g. Chave et
54 al. 2009, Kraft et al. 2010). The second approach implicitly assumes the optimal value for a
55 given trait changes across an environmental gradient. Thus, the two approaches appear to be
56 inconsistent, with the first searching for a single global optimum and the second searching for a
57 shifting optimum across an environmental gradient (Laughlin et al. 2018).

58 The functional diversity in ecological communities can potentially be explained by the
59 existence of alternative designs, *i.e.*, different phenotypic trait combinations that lead to similar
60 demographic performance in a given environment (Marks and Lechowicz 2006). Alternative

61 designs arise when the relationship between a trait and performance is dependent upon an
62 interaction with another trait. These trait-trait interactions can be demonstrated using
63 performance landscapes where one can visualize expected performance along two trait axes (Fig.
64 1). While performance landscapes are rarely utilized in functional trait-based ecology,
65 evolutionary biologists have long utilized these landscapes beginning with Wright's adaptive
66 landscape of gene frequencies (Wright 1931, Wright 1932, Wright 1945), progressing from
67 Simpson's phenotypic landscape (Simpson 1944) to adaptive landscapes (Arnold et al. 2001).
68 Despite this existing literature and the recognition for decades that plant functional trait-based
69 ecology should focus more intently on trait-trait interactions (Ackerly et al. 2000, Marks and
70 Lechowicz 2006, Dwyer and Laughlin 2017a, D'Andrea et al. 2018), performance landscapes
71 have been largely ignored (but see Laughlin and Messier 2015, Dwyer and Laughlin 2017b) as
72 has a focus on individual-level positions on these landscapes over that of species means.

73 Functional diversity within a community can be further promoted if the shape of
74 performance landscapes shifts along local-scale environmental gradients. In other words, the
75 alternative phenotypic designs that perform best on one end of a local-scale environmental
76 gradient will not necessarily be those expected to perform best on the other end thereby
77 increasing the diversity of traits and trait combinations performing well within a community
78 (Fig. 1). Thus, not only do trait-trait interactions need to be considered when modeling individual
79 performance, but a simultaneous investigation of the interactions among multiple traits and
80 environmental gradients may be necessary to understand how traits drive performance and plant
81 community diversity.

82 Theory indicates that trait-trait and trait-environment interactions are essential for
83 understanding how traits relate to whole-plant performance, influence population level
84 parameters, and drive community structure and dynamics (Marks and Lechowicz 2006, Enquist
85 et al. 2015). However, we currently lack clear empirical evidence that multiple phenotypic
86 optima exist in a given environment and that these optima change across an environmental
87 gradient. Ideally, such evidence would be gathered using individual-level trait, demographic and
88 environmental information to account for the importance of intraspecific trait variation (Yang et
89 al. 2018, Swenson et al. 2020). Here, we determined whether interactions between multiple
90 functional traits and environmental gradients impacted tropical tree seedling growth rates.
91 Specifically, we modeled the growth of 1,559 individual tree seedlings from 122 species in a

92 Chinese tropical rainforest using an unprecedented dataset of individual-level leaf, root, and stem
93 trait data and detailed light and soil nutrient data. We asked two main questions: 1) Do
94 alternative phenotypic designs have similar demographic outcomes within an environment?, and
95 2) how do the peaks and ridges of growth performance landscapes change across environmental
96 gradients? We focus on seedlings because differential demographic rates at the seedling stage
97 have large and lasting impacts on tropical forest structure and dynamics (Metz et al. 2010; Paine
98 et al. 2012; Green et al. 2014; Umaña et al. 2016).

99

100 **Methods**

101 *Study Site*

102 This study was conducted in a tropical rainforest in Xishuangbanna, which is in the
103 Chinese province of Yunnan (101°34'E, 21°36'N). The climate for this region is monsoonal with
104 a mean annual temperature of 21.8°C, mean annual precipitation of 1,493 mm, and soil pH
105 between 4.5 and 5.7 (Cao et al. 2008). There are two seasons in this forest, differentiated by
106 precipitation patterns, where the dry season starts in November and ends in April and 85% of the
107 precipitation occurs between May and October (Cao et al. 2008).

108

109 *Seedling Plot Establishment and Monitoring*

110 Across 2-ha of forest, 215 1 × 1 m² seedling plots were installed in a regular grid. All
111 seedlings from germination to 50 cm in height were tagged, identified, and monitored for 1 year
112 from 2013 to 2014. Seedlings were monitored for survival monthly, but height was measured
113 twice, once at the beginning and once at the end of the census period. During our study, the
114 average temperature was 22.4°C and the total rainfall was 1,590 mm. At the end of the year-long
115 monitoring, all surviving seedlings were harvested for functional trait measurement. In total,
116 there were 1,559 seedlings of 122 species distributed across the 215 plots. The number of
117 seedlings varied from one to 33 across the plots with a mean number of 7.25 individuals and 1.76
118 species per plot.

119

120 *Functional Traits*

121 Seven functional trait measurements were taken on each individual seedling in the study
122 (Appendix S1: Table S1). The organ-level traits measured were leaf mass per unit area (LMA)

123 and mean leaf thickness, which were measured on one to three leaves for each individual. The
124 biomass allocation traits measured in this study were leaf area ratio (LAR; total plant leaf area
125 divided by whole plant dry mass), leaf mass fraction (LMF; total leaf dry mass divided by whole
126 plant dry mass), root mass fraction (RMF; total root mass divided by whole plant mass), stem
127 mass fraction (SMF; total stem dry mass divided by whole plant dry mass), and stem specific
128 length (SSL; stem length divided by dry stem mass), all according to (Poorter et al. 2012) and
129 previously reported in (Umaña et al. 2015). Leaves, roots and stems were manually separated in
130 the lab using hand pruners and dried in the oven for 72 h at 70 °C. These traits were chosen for
131 measurement because they represent major allocation tradeoffs at the organ and whole plant
132 levels that should impact growth performance. Specifically, LMA represents the leaf economics
133 spectrum (Reich et al. 1997, Wright et al. 2004) where species with high LMA have a
134 conservative strategy with long leaf lifespans, but lower mass-based photosynthetic rates and
135 species with low LMA values have a more acquisitive strategy with short leaf life spans and
136 higher mass-based photosynthetic rates. Leaf thickness is measured to indicate leaf mechanical
137 resistance to damage (Onoda et al. 2011). LAR and LMF reflect relative allocation to leaf tissue
138 and combined with LMA are often used in models of plant growth in functional ecology (Garnier
139 1991, Enquist et al. 2007, Poorter et al. 2012). RMF, SMF and SSL are indicative of allocation to
140 non-photosynthetic tissue. RMF and LMA were of particular interest to us as previous work has
141 indicated that they both are highly responsive to soil nutrient and light gradients (Freschet et al.
142 2015). Higher RMF and higher LMA values indicate an allocation pattern that maximizes soil
143 resource gain relative to light resource gain. Thus, we might expect high RMF and LMA values
144 for individuals in poor soils and/or in shade tolerant individuals and the opposite pattern in
145 nutrient rich soils and/or in high light environments.

146

147 *Environmental Variables*

148 Local environmental conditions were characterized by measuring soil nutrients and light
149 availability for each plot. Prior research has shown that these environmental variables vary
150 significantly, even at local scales (Hubbell et al. 1999; Baldeck et al. 2013; Umaña et al. 2018).
151 Percent canopy openness, measured using hemispherical photographs taken systemically with a
152 Nikon FC-E8 lens and a Nikon Coolpix 4500 camera, was used to determine light availability.
153 We do note that these measurements only capture canopy openness and, therefore, do not capture

154 individual plant light environments or changes in light environments through time, but they do
155 offer a quick and pragmatic approach for estimating the average light environment in a sample
156 plot. Photographs were taken with the camera 1 m above the ground before sunrise with cloudy
157 conditions between March and April 2014 for each seedling plot. The images were analyzed
158 using Gap Light Analyser software ([http://www.caryinstitute.org/science-program/our-](http://www.caryinstitute.org/science-program/our-scientists/dr-charles-d-canham/gap-light-analyzer-gla)
159 [scientists/dr-charles-d-canham/gap-light-analyzer-gla](http://www.caryinstitute.org/science-program/our-scientists/dr-charles-d-canham/gap-light-analyzer-gla)) (Appendix S1: Table S2).

160 We also measured soil nutrients for each of the plots due to prior research showing
161 relationships between soil nutrients, habitat associations and demography (Itoh et al. 2003;
162 Palmiotto et al. 2004; Russo et al. 2005; John et al. 2007; Russo et al. 2008). To analyze soil
163 nutrients, 50 g of topsoil (0-10 cm in depth) was collected from each of the corners of the plot.
164 After being air dried and sifted, the cation availability was determined using the Mehlich III
165 extraction method and atomic emission inductively coupled plasma spectrometry (AE-ICP).
166 Total nitrogen (N) and carbon (C) content were determined by total combustion using auto-
167 analyzer and pH measured with a pH meter. All soil analyses were conducted at the
168 Biogeochemical Laboratory at Xishuangbanna Tropical Botanical Garden (Appendix S1: Table
169 S2).

170 All functional trait and environmental variables were natural log-transformed and scaled
171 to a mean of 0. The dimensionality of the soil data was reduced using a principal component
172 analysis (PCA) (Appendix S1: Fig. S1). The first three orthogonal axes, explaining 78% of the
173 total soil variation, were used for further analyses (Appendix S1: Table S3). PC1 scores were
174 negatively associated with K, Mg and Zn, which are known to play major roles in
175 photosynthesis, growth, as well as seed and stem maturation (Terry and Ulrich 1974; Holste et al.
176 2011; Broadley et al. 2007). PC2 scores were negatively associated with Ca and P. Soil
177 phosphorous is the major limitation of these two elements as phosphorous deficiency is known to
178 have negative impacts on plant growth (Wissuwa 2003; Wright et al. 2004). PC3 scores were
179 negatively associated with C and N. Soil N is of particular interest as N is a key component of
180 RuBisCO and, therefore, a resource that can limit photosynthesis (Evans and Clarke 2019).

181 182 *Quantifying Growth Rates*

183 To determine the relative growth rate (RGR) of each seedling, the change in log-
184 transformed height was calculated for each individual as:

185
$$\text{RGR} = (\log(M_{t+\Delta t}) - \log(M_t)) / \Delta t$$

186 The variable M is the height at successive time steps t (Hoffmann and Poorter 2002). A
187 value of 1 was added to all observed RGR values and then the data were natural log-transformed
188 and scaled to a mean of 0 to approximate normality (Appendix S1: Table S1).

189
190 *Linear Mixed-Effects Model Description*

191 We built linear mixed-effects models of growth using a Bayesian approach ranging in
192 complexity from a single term to having a three-way interaction with a focus on addressing the
193 biological question of whether trait-trait, trait-environment or trait-trait-environment interactions,
194 which are frequently not considered, influence growth rates. Models were run for all pairwise
195 combinations of the seven functional traits and environmental variables for a total of 84 models.
196 In all models, RGR followed a lognormal distribution:

197
$$\log\text{RGR}_i \sim N(z_i, \sigma_z)$$

198 where z_i was the relative growth rate of each individual, σ_z was the variance, and i was each
199 individual. First, individual linear models were fit where RGR was a function of a single trait and
200 initial seedling size, where z_i was the relative growth rate of each individual, α was the model
201 intercept, β_{1p} and β_{2j} were the plot and species random effects, respectively, β_3 was the effect
202 of a trait, β_4 was the effect of initial size.

203
$$z_i = \alpha + \beta_{1p} + \beta_{2j} + \beta_3 \times \text{trait} + \beta_4 \times \text{initial size} \quad (1)$$

204 These simple linear models highlight a common method used to link functional traits,
205 demographic rates, and population and community structure in the functional trait literature. In
206 rare instances, a functional trait and the environment have been combined in models to include
207 their interactive effect as both impact plant performance (Laughlin and Messier 2015, Dwyer and
208 Laughlin 2017b, Blonder et al. 2018). To mimic these models, we modeled the linear predictor,
209 RGR, using mixed-effects models including a two-way interaction between a functional trait and
210 an environmental variable. Models were of the general form,

211
$$z_i = \alpha + \beta_{1p} + \beta_{2j} + \beta_3 \times \text{trait} + \beta_4 \times \text{environment} + \beta_5 \times \text{initial size} + \beta_6$$

212
$$\times \text{trait} \times \text{environment} \quad (2)$$

213 where z_i was the relative growth rate of each individual, α was the model intercept, β_{1p} and β_{2j}
214 were the plot and species random effects, respectively, β_3 was the effect of a trait, β_4 was the

215 effect of the environmental variable, β_5 was the effect of initial seedling size, and β_6 was the
216 effect of the interaction between the trait and the environmental variable on RGR.

217 Lastly, we modeled RGR using a linear mixed-effects model including a three-way
218 interaction between two functional traits and an environmental variable. The three-way
219 interaction term in these models is included to represent a relationship between a functional trait
220 and growth performance dependent upon another functional trait and the environment. In this
221 model, RGR of each individual was modelled using the general form,

$$222 \quad z_i = \alpha + \beta_{1p} + \beta_{2j} + \beta_3 \times \text{trait}_1 + \beta_4 \times \text{trait}_2 + \beta_5 \times \text{environment} + \beta_6 \times \\ 223 \quad \text{trait}_1 \times \text{trait}_2 + \beta_7 \times \text{trait}_1 \times \text{environment} + \beta_8 \times \text{trait}_2 \times \text{environment} + \beta_9 \times \text{trait}_1 \times \\ 224 \quad \text{trait}_2 \times \text{environment} + \beta_{10} \times \text{initial size} \quad (3)$$

225 where z_i was the relative growth rate of each individual, α was the model intercept, β_{1p} and β_{2j}
226 were the plot and species random effects, respectively, β_3 was the effect of trait1, β_4 was the
227 effect of trait2, β_5 was the effect of the environmental variable, β_6 was the effect of the
228 interaction between trait1 and trait2, β_7 was the effect of the interaction between trait1 and the
229 environment, β_8 was the effect of the interaction between trait2 and the environment, β_9 was the
230 effect of the three-way interaction between trait1, trait2 and the environment, and β_{10} was the
231 effect of the initial seedling size on RGR.

232 In all models, plot (β_{1p}) and species (β_{2j}) were modeled as normally distributed random
233 intercepts to account for species-level differences in RGR that were unrelated to spatial
234 autocorrelation and the traits, respectively. For the hyperparameters of the random effects, we
235 specified diffuse normal priors: $N(\text{mean} = 0, \text{precision} = 0.01)$. The variance hyperparameters
236 were given diffuse gamma priors: $\text{Gamma}(\text{shape} = 0.1, \text{rate} = 0.1)$. We performed variable
237 selection by comparing “full” models, equation (3), with models of all other iterations of
238 variables using deviance information criterion (DIC) to determine the most parsimonious model
239 (Spiegelhalter et al. 2002). Typically, it is thought that DIC is a Bayesian analogue of AIC (Kéry
240 2010). They have a similar justification, but DIC has wider applicability (Spiegelhalter et al.
241 2002). The two main differences between AIC and DIC calculations are that the maximum
242 likelihood estimate is replaced with the posterior mean and the number of parameters is replaced
243 with a data-based bias correction (Gelman et al. 2013). Any model with a DIC value within 5
244 ($\Delta\text{DIC} < 5$) of the lowest value for all models was given consideration (Spiegelhalter et al. 2002;

245 Lesaffre and Lawson 2012). Along with evaluating models with DIC, we assessed the fit of the
246 models by checking the posterior predictive distribution of the fit of the actual data with the fit of
247 an “ideal” dataset and computed the Bayesian p -value (Gelman et al. 1996). As the Bayesian p -
248 value approaches 0.5, simulated data generated from the posteriors should look similar to the
249 observed data indicating a good fit model (Gelman et al. 2013). Evaluating models using DIC
250 and Bayesian p -values allowed us to compare less complex, commonly used models, equation
251 (1) for one, to our high-dimensional models (equations 2 and 3) to test for overall model fit
252 (Bayesian p -value ~ 0.5) and discover instances where more complex models, those containing a
253 three-way interaction, are more parsimonious ($\Delta\text{DIC} < 5$) than more simple models lacking a
254 three-way interaction between two traits and the environment. Pearson’s product-moment
255 correlation coefficients showed that some traits were weakly correlated (Appendix S1: Table
256 S4). We checked for multicollinearity between traits using variance inflation factor (VIF)
257 analysis to verify that all trait combinations had a VIF < 10 thereby indicating that we can
258 include them together in our models (Ohlemüller et al. 2006; Hair et al. 2014; Enquist et al.
259 2015) (Appendix S1: Table S4).

260 All models were fit using Markov Chain Monte Carlo (MCMC) sampling techniques in
261 *JAGS* 4.3.0 (Plummer 2003) interfaced with R v3.3.1 programming language using the *rjags*
262 (Plummer 2016) and *runjags* (Denwood 2016) packages (Data S1). We ran six parallel chains
263 with random initial values for 50,000 iterations with a burn-in period of 10,000 iterations.
264 Parameter estimates and 95% credible intervals were obtained from the quantiles of the posterior
265 distribution. Parameters were statistically supported when their credible interval did not overlap
266 zero. Convergence of the MCMC chains was assessed visually in traceplots and using the
267 Gelman-Rubin convergence diagnostic to ensure values were less than 1.1 (Gelman and Rubin
268 1992).

269

270 *Assessing Growth Performance Peaks*

271 Two criteria had to be met in order to declare the presence of alternative designs in a
272 growth performance landscape. First, the two-way (trait-trait, trait-environment) or three-way
273 interaction (trait-trait-environment) term in the model had to be statistically supported with 95%
274 credible intervals around the parameter estimate not overlapping zero. Second, the slope of the
275 relationship between the traits and RGR, computed as the first partial derivative of the fitted

276 model, had to switch signs across the range of the environmental variable (Laughlin 2018,
277 Laughlin et al. 2018). A switch in sign indicates that the partial derivative passed through zero at
278 some point along the environmental gradient. This would be evidence that a “saddle” exists at
279 the intermediate environmental condition, due to the probability surface being pulled downward
280 (Laughlin et al. 2018). To verify that the slope was significantly different from zero, we
281 randomly sampled parameter estimates, with replacement, from the posterior distribution 1000
282 times and calculated the slope for each sample to determine 95% confidence intervals (Appendix
283 S1: Table S5).

284 To understand how the effect of two functional traits on RGR changes across the
285 environmental gradients, simple slopes and intercepts were calculated to visualize partial effects
286 and peaks in growth performance. The minimum and maximum observed values were used as
287 constants for the second trait and environmental variable during the calculation of the simple
288 slopes and intercepts. We also statistically tested for the presence of multiple growth
289 performance peaks at each end of the environmental gradients. We randomly sampled, with
290 replacement, from the posterior distribution 1000 times from each model. We then calculated
291 each of the simple slopes for each of the 1000 samples. We then determined the number of times
292 the slopes were different in sign for the two growth performance peaks at the same end of the
293 environmental gradient. An exact binomial test with a probability of success equal to 0.50 was
294 used to test for significant differences. In all cases, a p value of < 0.05 indicated the presence of
295 two simple slopes, meaning traits were combining in different ways at the same end of the
296 environmental gradient to achieve higher RGR (Appendix S1: Table S6). If the signs of the mean
297 values of the simple slopes were in the same direction for both growth performance peaks in an
298 environment, we were unable to show a statistical presence of one versus two peaks. All analyses
299 were performed in *R* statistical software version 3.3.1 (R Development Core Team 2016).

300

301 **Results**

302 The models in this study were designed based on biological interactions of functional
303 traits and the environment that are known or predicted in the literature (Wright et al. 2004,
304 Baraloto et al. 2010, Fortunel et al. 2012, Adler et al. 2014, Reich et al. 2014, Freschet et al.
305 2015, Liu et al. 2016). Eight models, out of 84 total, had evidence of multiple growth
306 performance peaks indicated by a significant three-way interaction in the model and a slope that

307 changed sign along the environmental gradient (Appendix S2). Five models, each with a
308 different three-way interaction term, were the most parsimonious or equally parsimonious based
309 on comparison of DIC values between each “full” model (equation 3) and simpler versions of
310 each model (Appendix S2: Tables S1-S5). For the remaining three models, the “full” model was
311 not the most parsimonious overall after variable selection, based on DIC, but was more
312 parsimonious than commonly used models, trait-growth rate and trait \times environment-growth
313 rate (Appendix S2: Tables S6-S8). All eight of these models had appropriate Bayesian p -values
314 (~ 0.5) indicating model fit and that values calculated from the simulated data are distributed
315 around the observed values (Appendix S2).

316

317 *Comparison of Model Types*

318 Each model was built to evaluate commonly used modeling methods (single trait-growth
319 rate models and trait \times environment-growth rate models) with high dimensional models
320 containing a three-way interaction between two functional traits and the environment. Below we
321 present an extended comparison between simple models and the “full” model for one of the eight
322 different significant three-way interactions found (LMA \times RMF \times light). We then present just
323 the interpretation of the “full” model for the remaining seven three-way interactions.

324 The “full” model, which contained the three-way interaction LMA \times RMF \times light, had
325 equally the highest support (lower DIC) than all iterations of variables of this “full” model
326 (Appendix S2: Table S1). We compared the “full” model with the simplest, commonly used
327 models that fit linear mixed-effects models with relative growth rate (RGR) as a function of each
328 trait. We found significant negative relationships between leaf mass per area (LMA) and RGR
329 (Appendix S1: Table S7) as well as between root mass fraction (RMF) and RGR (Appendix S1:
330 Table S7). However, neither of these models was as well supported as the “full” model based on
331 DIC (Appendix S2: Table S1). Next, we included a trait by environment interaction into the
332 linear mixed-effects models. The interaction between LMA and light was not significant (Fig.
333 2a) so the first criteria for evidence of growth performance peaks was not met (Fig. 2b).
334 However, the interaction between RMF and light was significant (Fig. 2c), but the slope of the
335 relationship between RMF and RGR had only a few individuals cross zero along the light
336 gradient suggesting a weak interaction. There was one obvious peak in RGR for individuals
337 when they had low RMF in high light environments, however some individuals did occupy an

338 alternative peak where individuals had high RMF in low light environments (Fig. 2d). Despite
339 these models with two-way interactions showing evidence of growth peaks, they had higher DIC
340 values (less support) than the “full” model that contained the three-way interaction (Appendix
341 S2: Table S1). Furthermore, the single term and two-way interaction term models afforded less
342 interpretation of the effects of the model variables on growth because they lack the three-way
343 interaction term between two traits and the environment.

344 This “full” model contained a significant interaction between LMA, RMF, and light and
345 had equally the highest support (lowest DIC) following variable selection of the model (Fig. 3a;
346 Appendix S2: Table S1). The slope of the relationship between LMA and RGR at different
347 values of RMF changed sign along the light gradient indicating multiple growth performance
348 peaks which allows for the effect of the three-way interaction term on growth to be examined. In
349 low light environments, there were two growth performance peaks for individuals, one when
350 they had low LMA and high RMF and one when they had high LMA and low RMF (Fig. 3b). In
351 high light environments, there were also two growth performance peaks for individuals, one
352 when they had both high LMA and RMF and one when they had both low LMA and RMF (Fig.
353 3b).

354

355 *Evidence of Multiple Growth Performance Peaks*

356 The following three models had a three-way interaction term that was significant in the
357 model and had a slope that changed sign along the environmental gradient (i.e. multiple growth
358 performance peaks present). Variable selection was performed on each model separately using
359 DIC. For each of these models, the “full” model was not the best supported overall, but had
360 higher support than commonly used trait-growth rate and trait \times environment-growth rate
361 models (Appendix S2: Tables S6-S8). For each of these three models, the best supported model
362 was a complex model highlighting the inability of simple models to reflect the effects of the
363 traits and the environment on growth (Appendix S2: Tables S6-S8).

364 The first of these three models had a significant three-way interaction between LMA,
365 stem mass fraction (SMF) and light (Appendix S1: Fig. S2a; Appendix S2: Table S6). For
366 individuals to achieve a growth performance peak across the light gradient, they combined LMA
367 and SMF in different manners (Appendix S1: Fig. S2b). In low light environments, there were
368 two growth performance peaks for individuals, one when they have both low LMA and SMF and

369 one when they have both high LMA and SMF. In high light environments, there were also two
370 growth performance peaks for individuals, one when they have low LMA and high SMF and one
371 when they have high LMA and low SMF. The last two models involved three-way interactions
372 with the soil PC2 environmental variable, which was negatively associated with soil Ca and P.
373 The first involved an interaction between LMA, RMF and soil PC2 (Appendix S1: Fig. S3a;
374 Appendix S2: Table S7). When soil PC2 was low, indicating high levels of Ca and P, plants with
375 high LMA and low RMF or low LMA and high RMF grew faster (Appendix S1: Fig. S3b). In
376 high soil PC2 environments, indicating low levels of Ca and P, plants with either low LMA and
377 low RMF or high LMA and high RMF performed best (Appendix S1: Fig. S3b). Finally, there
378 was a significant interaction between leaf area ratio (LAR) and leaf mass fraction (LMF)
379 (Appendix S1: Fig. S4a; Appendix S2: Table S8). We found that the effect of LAR on growth
380 rates along the soil PC2 gradient was dependent on LMF (Appendix S1: Fig. S4b). In order for
381 individuals to be on a growth performance peak in low soil PC2 environments, meaning high Ca
382 and P, they had high LAR and low LMF or high LAR and high LMF (Appendix S1: Fig. S4b).
383 However, we were unable to statistically show each of these peaks separately because the slopes
384 for each peak were the same sign since LAR was high for both peaks. In high soil PC2
385 environments, individuals with high LAR and high LMF or low LAR and low LMF exhibited
386 peak growth performance (Appendix S1: Fig. S4b).

387 The “full” model of the remaining four models had the best support or equal support
388 ($\Delta DIC < 5$) after variable selection (Appendix S2: Table S2-S5). These models also had support
389 for multiple growth performance peaks (i.e. they had a slope that switched sign along the
390 environmental gradient). Three of these models had significant interactions of traits with soil
391 PC1, which was negatively associated with Mg, K, and Zn (Appendix S1: Table S3). The first
392 interaction was between LMA and RMF (Appendix S1: Fig. S5a; Appendix S2: Table S2). In
393 low soil PC1 environments, indicating high levels of Mg, K and Zn, individuals had high LMA
394 and low RMF or low LMA and high RMF (Appendix S1: Fig. S5b). In high soil PC1
395 environments, individuals with high LMA and high RMF or low LMA and low RMF exhibited
396 peak growth performance (Appendix S1: Fig. S5b). The second interaction was between leaf
397 thickness and RMF (Appendix S1: Fig. S6a; Appendix S2: Table S3). In order for individuals to
398 be on a growth performance peak in low soil PC1 environments, they had high leaf thickness and
399 low RMF or low leaf thickness and high RMF (Appendix S1: Fig. S6b). In high soil PC1

400 environments, individuals with high leaf thickness and high RMF or low leaf thickness and low
401 RMF exhibited peak performance (Appendix S1: Fig. S6b). The next interaction was between
402 leaf thickness and SMF (Appendix S1: Fig. S7a; Appendix S2: Table S4). Two performance
403 peaks were found when soil PC1 is low and when soil PC1 is high (Appendix S1: Fig. S7b).
404 When soil PC1 was low, indicating high levels of Mg, K and Zn, individuals with low leaf
405 thickness and low SMF or high leaf thickness and high SMF exhibited the highest RGR
406 (Appendix S1: Fig. S7b). When soil PC1 was high, indicating low values of Mg, K, and Zn,
407 individuals with low leaf thickness and high SMF or high leaf thickness and low SMF exhibited
408 peak growth performance (Appendix S1: Fig. S7b). The final model had a significant interaction
409 between leaf thickness, SSL, and soil PC2 (Appendix S1: Fig. S8a; Appendix S2: Table S5). For
410 this interaction of traits, peak growth performance in low soil PC2 environments occurred for
411 individuals that had high leaf thickness with high SSL or had low leaf thickness with low SSL
412 (Appendix S1: Fig. S8b). To perform well in high soil PC2 environments, plants with low leaf
413 thickness and high SSL or high leaf thickness and low SSL had faster growth (Appendix S1: Fig.
414 S8b).

415

416 **Discussion**

417 Here, we have provided empirical evidence of multiple peaks in growth rate, a strong
418 determinant of long-term plant performance, across phenotypic space in a diverse tropical
419 seedling community thereby indicating the presence of multiple successful alternative designs. In
420 other words, multiple trait combinations can lead to similar growth performance. The location of
421 growth performance peaks in phenotypic space shifts across local-scale light and soil gradients
422 such that no single or set of interacting traits resulted in a peak in growth across these
423 environmental gradients. These results help to demonstrate how functional diversity can be
424 maintained in ecological communities and question the practice of utilizing a single trait or
425 environmental variable in isolation to predict the growth performance of individual trees.

426 Through a step-wise process of increasing model complexity, we have shown that including
427 interactions between two functional traits and the environment and visualization of growth
428 performance landscapes leads to a better overall indication of how functional traits and the
429 environment affect individual seedling growth performance. Specifically, we provide five
430 separate instances where multiple growth performance peaks are found in best supported (Δ DIC

431 < 5) high-dimensional models containing a three-way interaction (Fig. 3, Appendix S1: Figs. S5-
432 S8).

433 Based on fast-slow plant economics theory (Reich 2014), it may be expected that single
434 growth performance peaks relating to a combination of acquisitive values may be found in areas
435 with higher resource levels. For example, species with relatively more leaf mass investment and
436 lower leaf mass per area (LMA) may be expected in high light environments (Lusk et al. 2008).
437 Similarly, combinations of conservative traits (e.g. low root mass investment and high LMA),
438 may be expected to have superior growth in resource poor (e.g. low light) environments. This
439 expectation is only partially supported by our results. For example, we did find a growth
440 performance peak for plants with acquisitive traits (i.e. relatively high root investment and low
441 LMA) in high soil nutrient environments (Appendix S1: Fig. S3, Fig. S5). However, we also
442 have several instances where multiple growth performance peaks occur at a given point on light
443 or soil gradients and many of these peaks combine an acquisitive below ground strategy and a
444 conservative above ground or leaf level strategy. For instance, at the high end of the soil PC1
445 gradient, meaning low levels of Mg, K, and Zn, growth performance peaked at either high LMA
446 with high root mass fraction (RMF), which reflect a more conservative leaf strategy and
447 acquisitive root strategy, respectively, or low LMA with low RMF, which reflect a more
448 acquisitive leaf strategy and conservative root strategy (Appendix S1: Fig. S5). For the soil
449 nutrient gradients, we found multiple growth performance peaks at both ends of the gradients.
450 The high ends of the soil PC1 and PC2 gradients were associated with low levels of K, Mg, Zn
451 (PC1) and Ca and P (PC2), nutrients known to play major roles in photosynthesis, growth, as
452 well as seed and stem maturation (Terry and Ulrich 1974; Wissuwa 2003; Wright et al. 2004;
453 Broadley et al. 2007; Holste et al. 2011). Soil moisture may have also contributed to peaks
454 associated with soil nutrients, but we were unable to measure this environmental axis.

455 This modulation of root and leaf resource acquisition may indicate a fourth interaction
456 between light and soil nutrient levels (Freschet et al. 2015). We did not explicitly test for
457 interactions between environmental gradients here, however, our results generally indicate that
458 above ground resource levels (i.e. light) and below ground resource levels (i.e. soil nutrients) can
459 vary independently such that mixtures of conservative and acquisitive leaf and root strategies can
460 be selected independently in a forest depending on the resource that is most limiting. Indeed, soil
461 and light variables are very weakly correlated in this study, which likely promotes a greater

462 diversity of trait combinations in the community (Appendix S1: Table S8). We do note that leaf
463 and root traits, at the plant level, are not independent of one another, given that plants only have
464 a finite amount of resources to invest in each. However, we have shown that plants can express
465 acquisitive leaf traits while their root traits are conservative, which may allow us to see
466 disassociation of leaf and root traits at the population or community level. Thus, our results often
467 did not indicate superior growth arising from either conservative or acquisitive strategies at the
468 whole plant scale and this is likely due to the independence of the selective environments above
469 and below ground in the system. In other systems where resource levels above and below ground
470 co-vary, a whole plant coordination of plant functional spectra may be more common (e.g.
471 Freschet et al. 2015). The results also coincide with evidence in the literature that indicates major
472 functional spectra (e.g. leaf and wood economics spectra (e.g. Baraloto et al. 2010); leaf and root
473 economics spectra (e.g. Fortunel et al. 2012)) are generally weakly correlated in adult trees in
474 tropical forests as is the case in the present study for tropical seedlings (Appendix S1: Table S4).
475 All other significant interactions were similar in that multiple growth performance peaks and
476 frequent independence of above and below ground strategies were evident (Appendix S1: Figs.
477 S2-S8).

478 Functional trait-based studies of plant community assembly and structure often focus on
479 abiotic selection for optimal trait values. For example, community weighted mean trait values are
480 expected to shift predictably across abiotic gradients (Muscarella and Uriarte 2016), and the
481 stress gradient hypothesis (Keddy 1992) emphasizes that the expected variation around this trait
482 optimum should decrease in more abiotically stressful conditions (Dwyer and Laughlin 2017b).
483 Correlative studies of plant functional traits and demographic rates implicitly assume that a
484 single trait value will lead to a similar demographic outcome across environments (Laughlin
485 2018; but see Westerband and Horvitz 2017). This is because of their use of a linear model
486 regressing a trait on a rate using data from many environments or datasets. We have shown
487 empirically that multiple growth performance peaks associated with different trait combinations
488 can occur at multiple points along an environmental gradient. Multiple growth performance
489 peaks were found on both ends of the environmental gradients, indicating that in extreme ends of
490 an environmental gradient, multiple trait combinations can lead to high demographic
491 performance. Importantly, we show the performance of a single trait value is dependent upon
492 other trait values. Combined, the trait-trait and trait-environment interactions, the context

493 dependencies of trait-performance relationships, and the ability of multiple trait combinations to
494 give rise to similar performance outcomes indicate why single functional traits often fail to
495 predict tree demographic rates (Poorter et al. 2008; Paine et al. 2015, Yang et al. 2018; Swenson
496 et al. 2020) and how trait diversity can be maintained in ecological communities.

497 High-dimensional trait-based trade-offs have been hypothesized as being important for
498 promoting species co-existence and maintaining community diversity (e.g. Adler et al. 2013,
499 Kraft et al. 2015). Our results support this hypothesis by showing that the relationship between
500 traits, the environment, and demographic outcomes is complex and can lead to alternative
501 phenotypic designs. While we find evidence in this study from multiple models of multiple
502 growth performance peaks, we understand that performance will vary across years and that
503 growth isn't the only metric of performance. We also know that the number of peaks we found is
504 relatively small compared to the number of species in our study system with only eight of 84
505 models having evidence of multiple growth performance peaks. This raises several new
506 questions that should be addressed in the future. First, how densely occupied are growth
507 performance peaks? Specifically, if multiple peaks exist in phenotypic space, are some more
508 densely occupied by individuals and species in the system and, if so, why? Second, are growth
509 performance peaks mitigated or eroded by other demographic outcomes (e.g. low survival rates,
510 recruitment or reproductive output) at the same or later life stages such that ultimately a single
511 peak is produced from a given environment? Answering these two questions is critical for our
512 understanding of why trait distributions in tropical forests often have only one or two modes (e.g.
513 Swenson et al. 2012). Final outstanding questions are: how do species that occupy the same
514 growth performance peak co-exist? Are intra-specific interactions (e.g. shared enemies,
515 competition) strong enough to permit the co-existence of multiple species on a given growth
516 performance peak? Do species occupying the same peak spatially or temporally segregate the
517 environment? These questions are all large foundational questions in trait-based community
518 ecology and our results should re-focus this literature towards a stronger consideration of
519 performance landscapes and multiple alternative phenotypic designs.

520

521 **Conclusions**

522 Here we have explored the possibility that multiple growth performance peaks occur in
523 the phenotypic space found in a diverse tropical seedling community using detailed individual

524 level trait and growth rate data. We find evidence for multiple peaks in phenotypic space and that
525 these peaks shift across environmental gradients. Further, we found evidence that above and
526 below ground functional strategies often combine to produce optimal growth performance in
527 such a way that acquisitive above ground strategies can align with conservative below ground
528 strategies and vice versa. Combined, these results show that there are multiple trait combinations
529 possible in phenotypic space that will lead to increased growth performance in a diverse
530 community, which lead to the promotion and maintenance of functional diversity. The results
531 also caution against focusing on single trait analyses in functional trait-based community ecology
532 and the aggregation of individual level trait variation to the species level. In particular, complex
533 trait-trait and trait-environment interactions are realized at the individual-level in communities
534 and performance landscapes should be empirically quantified and conceptualized using
535 individual-level data (Liu et al. 2016, Umaña et al. 2018, Swenson et al. 2020). Lastly, future
536 research will be needed to uncover the mechanisms that allow multiple species in a community
537 to occupy the same performance peaks in multidimensional phenotypic space and how above and
538 below ground resource levels interact to influence performance landscapes across systems.

539

540 **Acknowledgments**

541 This study was supported by NSF US-China Dimensions of Biodiversity grants to NGS (DEB-
542 1241136, DEB-1046113). The work was also supported by the Strategic Priority Research
543 Program of the Chinese Academy of Sciences (Grant Numbers XDB31000000 and XDPB0203),
544 the National Key R&D Program of China (2016YFC0500202) and the National Natural Science
545 Foundation of China (31370445, 31570430). This work was also supported by funding from the
546 University of Maryland and the US Department of Education GAANN program. Logistical
547 support was provided by Xishuangbanna Station of Tropical Rainforest Ecosystem Studies
548 (National Forest Ecosystem Research Station at Xishuangbanna), Chinese Academy of Sciences.
549 S.J.W., D.C.L. and N.G.S. generated the research idea; M.N.U., C.Z, L.L., M.C. and N.G.S.
550 organized and conducted data collection; S.J.W. analyzed data; and S.J.W., D.C.L. J.Z. and
551 N.G.S. wrote the paper with comments from all other authors.

552

553

554 **Literature Cited**

555 Ackerly, D. D. 2003. Community assembly, niche conservatism, and adaptive evolution in
556 changing environments. *International Journal of Plant Sciences* 164:S165-S184.

557 Ackerly, D. D., et al. 2000. The evolution of plant ecophysiological traits: Recent advances and
558 future directions. *BioScience* 50:979-995.

559 Adler, P. B., A. Fajardo, A. R. Kleinhesselink, and N. J. B. Kraft. 2013. Trait-based tests of
560 coexistence mechanism. *Ecology Letters* 16:1294-1306.

561 Adler, P. B., R. Salguero-Gómez, A. Compagnoni, J. S. Hsu, J. Ray-Mukherjee, C. Mbeau-Ache,
562 and M. Franco. 2014. Functional traits explain variation in plant life history strategies.
563 *Proceedings of the National Academy of Sciences USA* 111:740-745.

564 Anderson, J. T. 2016. Plant fitness in a rapidly changing world. *New Phytologist* 210:81-87.

565 Arnold, S. J., M. E. Pfrender, and A. G. Jones. 2001. The adaptive landscape as a conceptual
566 bridge between micro- and macroevolution. *Genetica* 112-113:9-32.

567 Baldeck, C. A., et al. 2013. Soil resources and topography shape local tree community structure
568 in tropical forests. *Proceedings of the Royal Society* 280:20122532.

569 Baraloto, C., C. E. T. Paine, L. Poorter, J. Beauchene, D. Bonal, A. Domenach, B. Hérault, S.
570 Patiño, J.-C. Roggy, and J. Chave. 2010. Decoupled leaf and stem economics in rain forest
571 trees. *Ecology Letters* 13:1338-1347.

572 Blonder, B., R. E. Kapas, R. M. Dalton, B. J. Graae, J. M. Heiling, and Ø. H. Opedal. 2018.
573 Microenvironment and functional-trait context dependence predict alpine plant community
574 dynamics. *Journal of Ecology* 106:1323-1337.

575 Broadley, M. R., P. J. White, J. P. Hammond, I. Zelko, and A. Lux. 2007. Zinc in plant. *New*
576 *Phytologist* 173:677-702.

577 Cao, M., H. Zhu, H. Wang, G. Lan, Y. Hu, S. Zhou, X. Deng, and J. Cui. 2008. Xishuangbanna
578 Tropical Seasonal Rainforest Dynamics Plot: Tree Distribution Maps, Diameter Tables and
579 Species Documentation. Yunnan Science and Technology Press, Kunming, China.

580 Cavender-Bares, J., D. D. Ackerly, D. A. Baum, and F. A. Bazzaz. 2004. Phylogenetic
581 overdispersion in Floridian oak communities. *American Naturalist* 163:823-843.

582 Chave, J., D. Coomes, S. Jansen, S. L. Lewis, N. G. Swenson, and A. E. Zanne. 2009. Towards
583 a worldwide wood economics spectrum. *Ecology Letters* 12:351-366.

584 Costa, D. S., F. Gerschlauer, H. Pabst, A. Kühnel, B. Huwe, R. Kiese, Y. Kuzyakov, and M.
585 Kleyer. 2017. Community-weighted means and functional dispersion of plant functional

586 traits along environmental gradients on Mount Kilimanjaro. *Journal of Vegetation Science*
587 28:684-695.

588 D'Andrea, R., A. Ostling, and J. P. O'Dwyer. 2018. Translucent windows: how uncertainty in
589 competitive interactions impacts detection of community pattern. *Ecology Letters* 21:826-
590 835.

591 Denwood, M. J. 2016. runjags: An R package providing interface utilities, model templates,
592 parallel computing methods and additional distributions for MCMC models in JAGS. *Journal*
593 *of Statistical Software* 71:1-25.

594 Dwyer, J. M., and D. C. Laughlin 2017a. Selection on trait combinations along environmental
595 gradients. *Journal of Vegetation Science* 28:672-673.

596 Dwyer, J. M. and D. C. Laughlin. 2017b. Constraints on trait combinations explain climatic
597 drivers of biodiversity: the importance of trait covariance in community assembly. *Ecology*
598 *Letters* 20:872-882.

599 Enquist, B. J., A. J. Kerkhoff, S. C. Stark, N. G. Swenson, M. C. McCarthy, and C. A. Price.
600 2007. A general integrative model for scaling plant growth, carbon flux, and functional trait
601 spectra. *Nature* 449:218-222.

602 Enquist, B. J., J. Norberg, S. P. Bonser, C. Violle, C. T. Webb, A. Henderson, L. L. Sloat, and V.
603 M. Savage. 2015. Scaling from traits to ecosystems: Developing a general trait driver theory
604 via integrating trait-based and metabolic scaling theories. *Advances in Ecological Research*
605 52:249-318.

606 Evans, J. R., and V. C. Clarke. 2019. The nitrogen cost of photosynthesis. *Journal of*
607 *Experimental Botany* 70:7-15.

608 Fonseca, C. R., J. M. C. Overton, B. Collins. and M. Westoby. 2000. Shifts in trait-combinations
609 along rainfall and phosphorus gradients. *Journal of Ecology* 88:964-977.

610 Fortunel, C., P. V. A. Fine, and C. Baraloto. 2012. Leaf, stem and root tissue strategies across
611 758 Neotropical tree species. *Functional Ecology* 26:1153-1161.

612 Freschet, G. T., E. M. Swart, and J. H. C. Cornelissen. 2015. Integrated plant phenotypic
613 responses to contrasting above- and below-ground resources: key roles of specific leaf area
614 and root mass fraction. *New Phytologist* 206:1247-1260.

615 Garnier, E. 1991. Resource capture, biomass allocation and growth in herbaceous plants. *Trends*
616 *in Ecology and Evolution* 6:126-131.

617 Gelman, A., and D. B. Rubin. 1992. Inference from iterative simulation using multiple
618 sequences. *Statistical Science*. 7:457-511.

619 Gelman, A., X.-L. Meng, and H. Stern. 1996. Posterior predictive assessment of model fitness
620 via realized discrepancies. *Statistica Sinica* 6:733-807.

621 Gelman, A., J. B. Carlin, H. S. Stern, D. B. Dunson, A. Vehtari, and D. B. Rubin. 2013. *Bayesian*
622 *Data Analysis*, Third Edition. Chapman and Hall/CRC, New York, USA.

623 Green, P. T., K. E. Harms, and J. H. Connell. 2014. Nonrandom, diversifying processes are
624 disproportionately strong in the smallest size classes of a tropical forest. *Proceedings of the*
625 *National Academy of Sciences USA* 111:18649-18654.

626 Hair, J. F., W. C. Black, B. J. Babin, and R. E. Anderson. 2014. *Multivariate Data Analysis*,
627 *Seventh Edition*. Pearson Education Limited, Harlow, UK.

628 HilleRisLambers, J., P. B. Adler, W. S. Harpole, J. M. Levine, and M. M. Mayfield. 2012.
629 Rethinking community assembly through the lens of coexistence theory. *Annual Review of*
630 *Ecology, Evolution, and Systematics* 43:227-248.

631 Hoffmann, W. A., and H. Poorter. 2002. Avoiding bias in calculations of relative growth rate.
632 *Annals of Botany* 80:37-42.

633 Holste, E. K., R. K. Kobe, and C. F. Vriesendorp. 2011. Seedling growth responses to soil
634 resources in the understory of a wet tropical forest. *Ecology* 92:1828-1838.

635 Hubbell, S. P., R. B. Foster, S. T. O'Brien, K. E. Harms, R. Condit, B. Wechsler, S. J. Wright,
636 and S. Loo de Lao. Light-gap disturbances, recruitment limitation, and tree diversity in a
637 Neotropical forest. *Science* 283:554-557.

638 Itoh, A., T. Yamakura, T. Ohkubo, M. Kanzaki, P. A. Palmiotto, J. V. LaFrankie, P. S. Ashton,
639 and H. S. Lee. 2003. Importance of topography and soil texture in the spatial distribution of
640 two sympatric dipterocarp trees in a Bornean rainforest. *Ecological Research* 18:307-320.

641 Jager, M. M., S. J. Richardson, P. J. Bellingham, M. J. Clearwater, and D. C. Laughlin. 2015.
642 Soil fertility induces coordinated responses of multiple independent functional traits. *Journal*
643 *of Ecology* 103:374-385.

644 John, R., J. W. Dalling, K. E. Harms, J. B. Yavitt, R. F. Stallard, M. Mirabello, S. P. Hubbell, R.
645 Valencia, H. Navarrete, M. Vallejo, and R. B. Foster. 2007. Soil nutrients influence spatial
646 distributions of tropical tree species. *Proceedings of the National Academy of Sciences USA*
647 104:864-869.

- 648 Keddy, P. A. 1992. Assembly and response rules: two goals for predictive community ecology.
649 *Journal of Vegetation Science* 3:157-164.
- 650 Kéry, M. 2010. Introduction to WinBUGS for ecologists. Academic Press, Burlington, USA.
- 651 Kraft, N. J. B., O. Godoy, and J. M. Levine. 2015. Plant functional traits and the
652 multidimensional nature of species coexistence. *Proceedings of the National Academy of*
653 *Sciences USA* 112:797-802.
- 654 Kraft, N. J. B., M. R. Metz, R. S. Condit, and J. Chave. 2010. The relationship between wood
655 density and mortality in a global tropical forest data set. *New Phytologist* 188:1124-1136.
- 656 Laughlin, D. C. 2018. Rugged fitness landscapes and Darwinian demons in trait-based ecology.
657 *New Phytologist* 217:501-503.
- 658 Laughlin, D. C., and J. Messier. 2015. Fitness of multidimensional phenotypes in dynamic
659 adaptive landscapes. *Trends in Ecology and Evolution* 30:487-496.
- 660 Laughlin, D. C., R. T. Strahan, P. B. Adler, and M. M. Moore. 2018. Survival rates indicate that
661 correlations between community-weighted mean traits and environments can be unreliable
662 estimates of the adaptive value of traits. *Ecology Letters* 21:411-421.
- 663 Lesaffre, E., and A. B. Lawson. 2012. Bayesian biostatistics. John Wiley & Sons, West Sussex,
664 UK.
- 665 Liu, X., N. G. Swenson, D. Lin, X. Mi, M. N. Umaña, B. Schmid, and K. Ma. 2016. Linking
666 individual-level functional traits to tree growth in a subtropical forest. *Ecology* 97:2396-
667 2405.
- 668 Lusk, C. H., P. B. Reich, R. A. Montgomery, D. D. Ackerly, and J. Cavender-Bares. 2008. Why
669 are evergreen leaves so contrary about shade? *Trends in Ecology and Evolution* 23:299-303.
- 670 Marks, C. O., and M. J. Lechowicz. 2006. Alternative designs and the evolution of functional
671 diversity. *American Naturalist* 167:55-66.
- 672 McGill, B. J., B. J. Enquist, E. Weiher, and M. Westoby. 2006. Rebuilding community ecology
673 from functional traits. *Trends in Ecology and Evolution* 21:178-185.
- 674 Metz, M. R., W. P. Sousa, and R. Valencia. 2010. Widespread density-dependent seedling
675 mortality promotes species coexistence in a highly diverse Amazonian rain forest. *Ecology*
676 91:3675-3685.
- 677 Muscarella, R., and M. Uriarte. 2016. Do community-weighted mean functional traits reflect
678 optimal strategies? *Proceedings of the Royal Society B: Biological Sciences* 283:20152434.

679 Ohlemüller, R., S. Walker, and J. B. Wilson. 2006. Local vs regional factors as determinants of
680 the invasibility of indigenous forest fragments by alien plant species. *Oikos* 112:493-501.

681 Onoda, Y., et al. 2011. Global patterns of leaf mechanical properties. *Ecology Letters* 14:301-
682 312.

683 Paine, C. E. T., M. Stenflo, C. D. Philipson, P. Saner, R. Bagchi, R. C. Ong, and A. Hector.
684 2012. Differential growth responses in seedlings of ten species of Dipterocarpaceae to
685 experimental shading and defoliation. *Journal of Tropical Ecology* 28:377-384.

686 Paine, C. E. T., et al. 2015. Globally, functional traits are weak predictors of juvenile tree
687 growth, and we do not know why. *Journal of Ecology* 103:978-989.

688 Palmiotto, P. A., S. J. Davies, K. A. Vogt, M. S. Ashton, D. J. Vogt, and P. S. Ashton. 2004.
689 Soil-related habitat specialization in dipterocarp rain forest tree species in Borneo. *Journal of*
690 *Ecology* 92:609-623.

691 Plummer, M. 2003. JAGS: A program for analysis of Bayesian graphical models using Gibbs
692 sampling. In: *Proceedings of the 3rd International workshop on distributed statistical*
693 *computing*.

694 Plummer, M. 2016. rjags: Bayesian graphical models using MCMC. R package version 4-6.
695 <https://CRAN.R-project.org/package=rjags>.

696 Poorter, H., K. J. Niklas, P. B. Reich, J. Oleksyn, P. Poot, and L. Mommer. 2012. Biomass
697 allocation to leaves, stems and roots: meta-analyses of interspecific variation and
698 environmental control. *New Phytologist* 193:30-50.

699 Poorter, L., et al. 2008. Are functional traits good predictors of demographic rates? Evidence
700 from five neotropical forests. *Ecology* 89:1908-1920.

701 R Development Core Team. 2016. R: A language and environment for statistical computing. R
702 Foundation for Statistical Computing, Vienna, Austria. <https://www.R-project.org/>.

703 Reich, P. B. 2014. The world-wide ‘fast-slow’ plant economics spectrum: a traits manifesto.
704 *Journal of Ecology* 102:275-031.

705 Reich, P. B., M. B. Walters, and D. S. Ellsworth, 1997. From tropics to tundra: Global
706 convergence in plant functioning. *Proceedings of the National Academy of Sciences USA*
707 94:13730-13734.

708 Russo, S. E., S. J. Davies, D. A. King, and S. Tan. 2005. Soil-related performance variation and
709 distributions of tree species in a Bornean rain forest. *Journal of Ecology* 93:879-889.

- 710 Russo, S. E., P. Brown, S. Tan, and S. J. Davies. 2008. Interspecific demographic trade-offs and
711 soil-related habitat associations of tree species along resource gradients. *Journal of Ecology*
712 96:192-203.
- 713 Simpson, G. G. 1944. *Tempo and Mode in Evolution*. Columbia University Press, New York,
714 USA.
- 715 Spiegelhalter, D. J., N. G. Best, B. P. Carlin, and A. Van Der Linde. 2002. Bayesian measures of
716 model complexity and fit. *Journal of the Royal Statistical Society Series B: Statistical*
717 *Methodology*. 64:583-616.
- 718 Swenson, N. G., et al. 2012. The biogeography and filtering of woody plant functional diversity
719 in North and South America. *Global Ecology and Biogeography* 21:798-808.
- 720 Swenson, N. G., S. J. Worthy, D. Eubanks, Y. Iida, L. Monks, K. Petprakob, V. E. Rubio, K.
721 Staiger, and J. Zambrano. 2020. A reframing of trait-demographic rate analyses for ecology
722 and evolutionary biology. *International Journal of Plant Sciences* 181.
- 723 Terry, N., and A. Ulrich. 1974. Effects of magnesium deficiency on the photosynthesis and
724 respiration of leaves of sugar beet. *Plant Physiology* 54:379-381.
- 725 Umaña, M. N., C. Zhang, M. Cao, L. Lin, and N. G. Swenson. 2015. Commonness, rarity, and
726 intraspecific variation in traits and performance in tropical tree seedlings. *Ecology Letters*
727 18:1329-1337.
- 728 Umaña, M. N., J. Forero-Montaña, R. Muscarella, C. J. Nytech, J. Thompson, M. Uriarte, J.
729 Zimmerman, and N. G. Swenson. 2016. Interspecific functional convergence and divergence
730 and intraspecific negative density dependence underlie the seed-seedling transition in tropical
731 trees. *The American Naturalist* 187:99-109.
- 732 Umaña, M. N., E. F. Zipkin, C. Zhang, M. Cao, L. Lin, and N. G. Swenson. 2018 Individual-
733 level trait variation and negative density dependence affect growth in tropical tree seedlings.
734 *Journal of Ecology* 106:2446-2455.
- 735 Westerband, A. C., and C. C. Horvitz. 2017. Early life conditions and precipitation influence the
736 performance of widespread understorey herbs in variable light environments. *Journal of*
737 *Ecology* 105:1298-1308.
- 738 Wissuwa, M. 2003. How do plants achieve tolerance to phosphorus deficiency? Small causes
739 with big effects. *Plant Physiology* 133:1947-1958.

740 Wright, I. J., and M. Westoby. 1999. Differences in seedling growth behavior among species:
741 trait correlations across species, and trait shifts along nutrient compared to rainfall gradients.
742 *Journal of Ecology* 87:85-97.

743 Wright, I. J., et al. 2004. The worldwide leaf economics spectrum. *Nature* 428:821-827.

744 Wright, S. 1931. Evolution in Mendelian populations. *Genetics* 16:97-159.

745 Wright, S. 1932. The roles of mutation, inbreeding, crossbreeding, and selection in evolution.
746 *Proceedings of the Sixth International Congress of Genetics* 1:356-366.

747 Wright, S. 1945. Tempo and mode in evolution: a critical review. *Ecology* 26:415-419.

748 Yang, J., M. Cao, and N. G. Swenson. 2018. Why functional traits do not predict trait
749 demographic rates. *Trends in Ecology and Evolution* 33:326-336.

750 **Data Availability**

751 All code and data associated with this study are available from
752 <http://doi.org/10.5281/zenodo.3382271>

753

754 **Figure Legends**

755 **Figure 1.** Conceptual model of a theoretical performance landscape of an individual along two
756 trait axes at (a) the low end of an environmental gradient and (b) at the high end of an
757 environmental gradient. Note the multiple performance peaks within an environment and the
758 shift in location of these performance peaks across the environmental gradient.

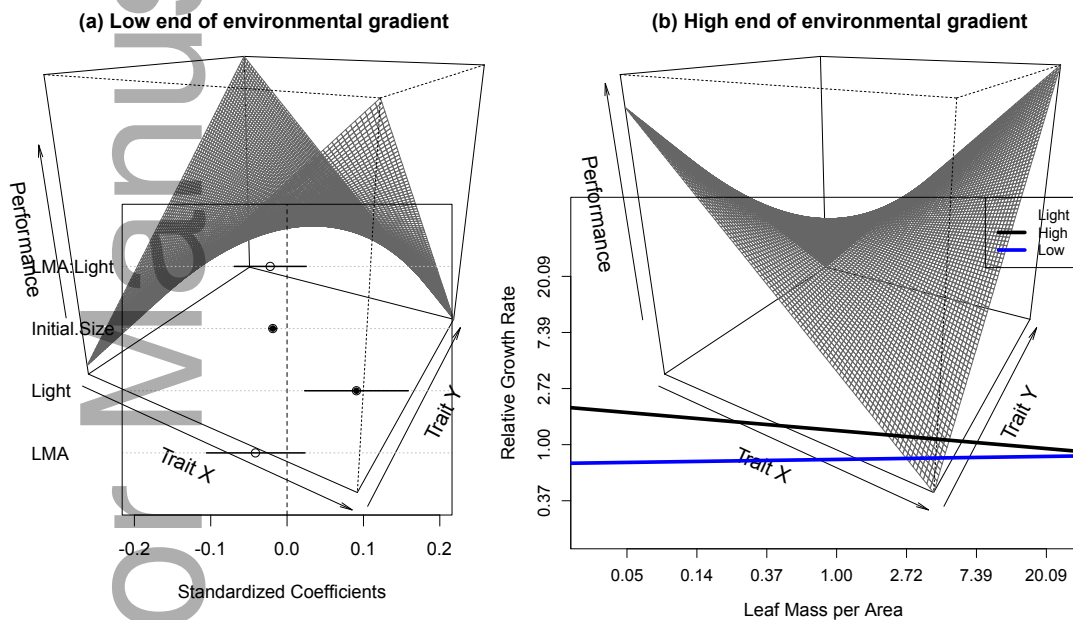
759 **Figure 2.** Models including two-way interactions between leaf mass per area (LMA) and light (a,
760 b) and between root mass fraction (RMF) and light (c, d). a,c) Standardized regression
761 coefficients where circles indicate posterior mean values, lines indicate 95% credible intervals,
762 and filled circles represent significant effects. b) Simple slopes and intercepts visualizing the
763 partial effects of LMA on RGR when light is held constant at its minimum (0.66) and maximum
764 values (10.10). d) Simple slopes and intercepts visualizing the partial effects of RMF on RGR
765 when light is held constant at its minimum (0.66) and maximum (10.10) values. All variables
766 were natural log-transformed and scaled to unit variance. Values on the axes have been back
767 transformed.

768 **Figure 3.** Model including three-way interaction between leaf mass per area (LMA), root mass
769 fraction (RMF), and light. a) Standardized regression coefficients where circles indicate posterior
770 mean values, lines indicate 95% credible intervals, and filled circles represent significant effects.

771 b) Simple slopes and intercepts visualizing the partial effects of LMA on RGR when RMF and
 772 light are held constant at combinations of their minimum (RMF = 0.04, Light = 0.66) and
 773 maximum (RMF = 0.93, Light = 10.10) values. All variables was scaled and natural log-
 774 transformed. Values on the axes have been back transformed. In low light environments, there
 775 are two growth performance peaks for individuals, one when they have low LMA and high RMF
 776 and one when they have high LMA and low RMF. In high light environments, there are two
 777 performance peaks for individuals, one when they have low LMA and low RMF and one when
 778 they have high LMA and high RMF.

779
 780
 781

Figure 1



782
 783
 784

Figure 3

